AIP Advances

RESEARCH ARTICLE | OCTOBER 10 2014

Determination of constitutive parameters of homogeneous metamaterial slabs by a novel calibration-independent method

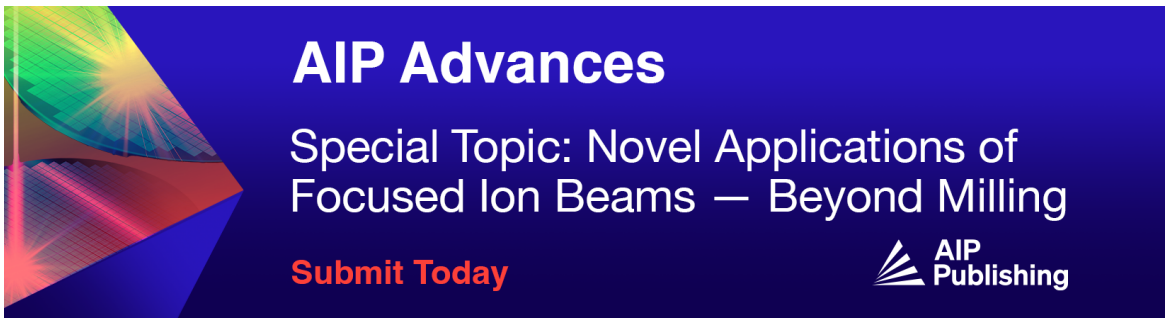
U. C. Hasar; G. Buldu; M. Bute; J. J. Barroso; T. Karacali; M. Ertugrul

Check for updates

AIP Advances 4, 107116 (2014)
https://doi.org/10.1063/1.4898148

View Online
Export Citation
CrossMark

24 December 2023 12:54:29



AIP Publishing

Determination of constitutive parameters of homogeneous metamaterial slabs by a novel calibration-independent method

U. C. Hasar,[1,2,a] G. Buldu,[1] M. Bute,[1] J. J. Barroso,[3] T. Karacali,[2,4] and M. Ertugrul[2,4]

[1]*Department of Electrical and Electronics Engineering, University of Gaziantep, Gaziantep 27310, Turkey*

[2]*Center for Research and Application of Nanoscience and Nanoengineering, Ataturk University, Erzurum 25240, Turkey*

[3]*Associated Plasma Lab., National Inst. for Space Research 12227-010 São José dos Campos, SP, Brazil*

[4]*Department of Electrical and Electronics Engineering, Ataturk University, 25240, Erzurum, Turkey*

(Received 2 July 2014; accepted 28 September 2014; published online 10 October 2014)

A calibration-independent line-line method for broadband and simultaneous constitutive parameters determination of homogeneous metamaterial (MM) slabs is proposed. It is shown that the sufficient condition for parameters retrieval by the proposed method is to measure uncalibrated (raw) complex scattering parameters of measurement cells (different air regions in free-space) which are completely and partially loaded by the two identical metamaterial slabs. The stability of derived equations for different measurement uncertainty cases is analyzed. We have validated the proposed method by using simulated scattering parameters of a MM slab with split-ring-resonators and then by comparing the extracted electromagnetic parameters with those of a general method used in the literature in the cases with and without a small offset in reference-plane positions (as well as other measurement errors). From this comparison, we note that while the general method does not eliminate those errors, the proposed method not only does not introduce the non-physical anti-resonance behavior but also removes the measurement errors arising from different mechanisms such as inaccurate reference-plane positions and mismatched connections. *© 2014 Author(s). All article content, except where otherwise noted, is licensed under a Creative Commons Attribution 3.0 Unported License.* [http://dx.doi.org/10.1063/1.4898148]

24 December 2023 12:54:29

I. INTRODUCTION

Materials characterization is an important research field involving an analysis of electromagnetic responses of various materials through the relative complex permittivity (ε_r), the relative complex permeability (μ_r), and other related parameters (e.g., magneto-electric coupling and chiral parameters). With the advent of artificial resonant-type structures (coined as metamaterials–MMs), it becomes possible to devise an engineered material with some exotic electromagnetic properties including negative refractive index (n) so that otherwise unattainable applications such as perfect lenses[1] and invisibility cloaks[2] come into real. The first fabricated MM was composed of periodic arrangement of a metallic-dielectric cell with split-ring-resonators (SRRs) and a thin metal wires on opposite faces of a dielectric substrate.[3] After this MM structure, various MM slabs have been proposed for different purposes, some of which are given.[4–7]

[a]Electronic mail: uchasar@gantep.edu.tr

 ©Author(s) 2014

In artificially constructed MM structures, both the size of the composite particles and the period of lattices are generally made larger than the wavelength at the particle resonance, and so a homogenized description[3] applies thus allowing the description of the properties of MMs in terms of bulk or macroscopic material parameters (ε_r and μ_r). In the literature, very interesting techniques have been proposed for retrieval of electrical properties of homogeneous MMs.[3,8–20] Many of these methods require some sort of calibration (named as calibration-dependent techniques) before accurate measurements are carried out.[3,8–17] However, calibration kits used for calibration of measurements may produce inappropriate material characterization due to inaccurate scattering (S-) parameter measurements arising from imperfect calibration kits. In recent studies, we have applied calibration-independent techniques[18–20] for accurate electromagnetic characterization of MMs. Nonetheless, these techniques are restricted to the measurement of either ε_r or μ_r.

It was shown that the complex propagation constant (γ) (as well as all the properties of an unknown transmission line and those of the junctions to the measurement lines) of a non-reflecting line can be determined from uncalibrated (raw) S-parameter measurements by a line-line (LL) method.[21–24] In this research paper, we propose a new calibration-independent method based on the LL technique for constitutive parameter (ε_r and μ_r) measurements of isotropic MM slabs.

II. THE METHOD

A. Background

Fig. 1 presents the measurement configurations of our method for retrieval of constitutive parameters of a homogeneous[3] MM slab with different lengths, L_1 and L_2. Here, the length of a MM slab refers to the length of the substrate in the propagation direction (in our analysis, it is the x direction as shown in Fig. 2(a)). More information about definition of the length of MM slabs can be found in Section IV. S_1 and S_2 denote the two-port networks for the slab region with different lengths (shorter and longer ones) to be determined; and X and Y designate two-port (error) networks corresponding to transitions used for linking S_1 and S_2 to a vector network analyzer (VNA) or a calibrated reference plane. In Fig. 1(a), the shorter slab with length L_1 is placed between two horn antennas, while the longer slab with length L_2 is positioned between the same antennas in Fig. 1(b). The final configuration, Fig. 1(c), illustrates the case when the shorter slab at arbitrary distances L_{01} and L_{02} replaces the longer one. In each measurement configuration, it is assumed that the regions where the slabs are positioned are at far field (zone) of the antennas (plane wave assumption) and that X and Y are asymmetrically spaced ($D_1 \neq D_2$) from each measurement cell. The networks X and Y include source and load match errors, errors due to mismatched connections, transitions between connecting cables and horn antennas, contact structures, embedded devices, etc. The methodology in calibration-independent techniques is to characterize S_1 and/or S_2 without resorting to any knowledge of error networks X and Y; that is, the effect of these networks has to be removed from the whole system.

B. Propagation constant determination

For the analysis of cascaded networks, either of the two transfer matrix forms, namely, ABCD[25–27] or wave cascading matrix (WCM)[18–20,28–30] can be employed. Because the WCM form is more useful for treating two-port calibration problems than the ABCD form,[28] in this paper, we will use the WCM form.

The basis for propagation constant determination in the LL technique (discussed in Section I) relies upon using two identical unknown MM slabs with different lengths L_u where $u = 1$ or 2 asymmetrically ($D_1 \neq D_2$) spaced from the antennas as schematized in Fig. 1(a) and Fig. 1(b).[21–24] We use the matrices T_X, T_Y, T_{L1} and T_{L2} for modeling, respectively, the transitions X, Y, and the measurement cells including slabs with different lengths. The WCM presentation of the whole system in Figs. 1(a) and (b) for two measurement cells loaded with slabs can be expressed as[18–20,28–30]

$$M_u = T_X T_{Lu} T_Y, \tag{1}$$

24 December 2023 12:54:29

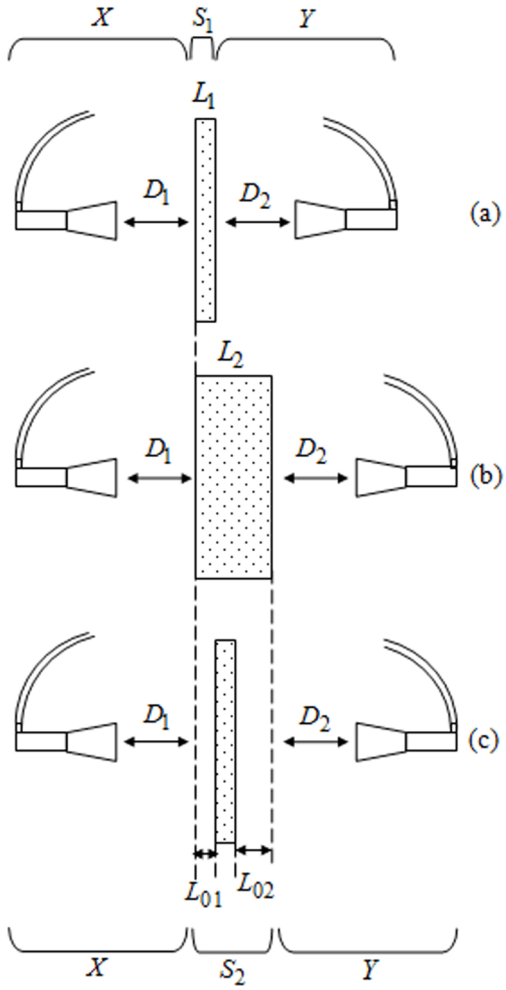


FIG. 1. Typical two-port measurement problem: unknown two-port network (S_1 and S_2) and two-port error networks, X and Y.

where

$$M_u = \frac{1}{S_{21}^{(u)}} \begin{bmatrix} S_{12}^{(u)} S_{21}^{(u)} - S_{11}^{(u)} S_{22}^{(u)} & S_{11}^{(u)} \\ -S_{22}^{(u)} & 1 \end{bmatrix}, \tag{2}$$

and $S_{kl}^{(u)}$ parameters $(k,l = 1,2)$ are the uncalibrated (raw) measured complex S-parameters. Using Eq. (2), the theoretical WCM form for T_{Lu} in Eq. (1) can be expressed as[18–20,29]

$$T_{Lu} = \frac{1}{(1-\Gamma^2)T_{su}} \begin{bmatrix} T_{su}^2 - \Gamma^2 & \Gamma\left(1 - T_{su}^2\right) \\ -\Gamma\left(1 - T_{su}^2\right) & 1 - \Gamma^2 T_{su}^2 \end{bmatrix}, \tag{3}$$

where

$$\Gamma = \frac{z-1}{z+1}, \quad T_{su} = e^{-\gamma L_u}, \quad z = z' + iz'' = \sqrt{\mu_r/\varepsilon_r}, \quad n = n' + in'' = \sqrt{\varepsilon_r \mu_r}, \tag{4}$$

$$\gamma = \gamma_0 n, \quad \gamma_0 = -i\frac{2\pi}{\lambda_0}, \quad \varepsilon_r = \varepsilon_r' + i\varepsilon_r'', \quad \mu_r = \mu_r' + i\mu_r''. \tag{5}$$

Here, γ, z, and n are, respectively, the propagation constant, normalized wave impedance, and refractive index of the slab-filled cell, and γ_0, μ_0, and λ_0 correspond to the propagation constant,

24 December 2023 12:54:29

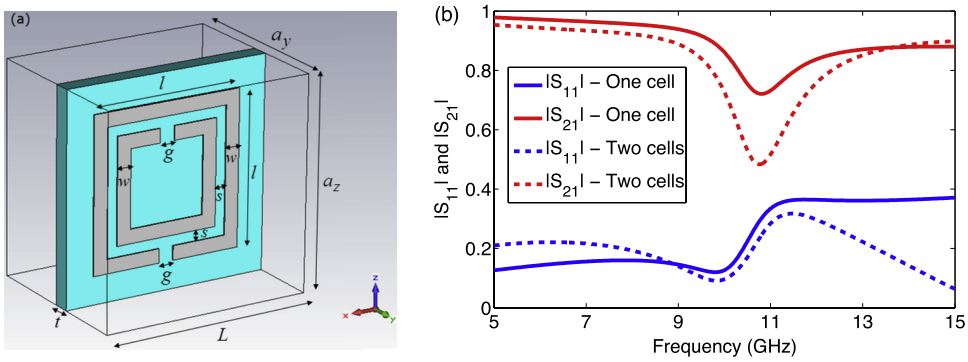


FIG. 2. (a) Configuration of the unit cell for the analyzed SRR MM slab (for better visualization, the substrate thickness and the dimensions of the metallic inclusions are not drawn to the scale of the cubic cell) and (b) magnitudes of simulated S-parameters of two MM slabs with $L_1 = 4.0$ mm (periodic arrangement of unit cell in y and z directions with periods $a_y = 4.0$ mm and $a_z = 4.0$ mm) and $L_2 = 8.0$ mm (cascade connection in the propagation (x) direction of two identical MM slabs with length L_1), corresponding to the configurations in Fig. 1(a) and 1(b), respectively.

permeability, and wavelength of free-space. In our mathematical analysis, $\exp(-i\omega t)$ time dependence has been assumed in phasor (complex) domain.

The theoretical WCM form for T_{Lu} given in Eq. (3) can be written in a different form[23] as

$$T_{Lu} = T_\Gamma T_{0u} T_\Gamma^{-1}, \tag{6}$$

where $*^{-1}$ denotes the inverse of the matrix '$*$' and

$$T_\Gamma = \begin{bmatrix} 1 & \Gamma \\ \Gamma & 1 \end{bmatrix}, \quad T_{0u} = \begin{bmatrix} T_{su} & 0 \\ 0 & T_{su}^{-1} \end{bmatrix}. \tag{7}$$

Using Eqs. (1), (6), and (7), we can write

$$M_1 M_2^{-1} = (T_X T_\Gamma)\left(T_{01} T_{02}^{-1}\right)(T_X T_\Gamma)^{-1}. \tag{8}$$

It is obvious from Eq. (8) that $M_1 M_2^{-1}$ and $T_{01} T_{02}^{-1}$ are similar matrices.[18–20,29] Using the fact that similar matrices have the same trace (denoted by Tr in the remainder of the manuscript), which is the sum of diagonal elements in a square matrix, and hence both matrices have the same eigenvalues, from Eq. (8) we obtain[22,23]

$$\lambda_{(1,2)} = \frac{Tr\left(M_1 M_2^{-1}\right) \mp \sqrt{\left[Tr\left(M_1 M_2^{-1}\right)\right]^2 - 4}}{2}, \tag{9}$$

where $\lambda_{(1,2)} = \exp(\mp\gamma \Delta L)$, $\Delta L = L_2 - L_1$, and λ represents either forward or backward traveling waves inside the slab. Finally, the propagation constant will be

$$\gamma_{(1,2)} = \mp \frac{\ln\left(\lambda_{(1,2)}\right)}{\Delta L}. \tag{10}$$

C. Constitutive parameters determination

The technique for determination of ε_r and μ_r of isotropic homogenized MM slabs by the proposed method is based upon using raw S-parameters measured on a given cell completely filled with a longer slab and then partially filled with a shorter slab as shown in Fig. 1(b) and Fig. 1(c).

The WCM form of the whole system for a measurement cell loaded by the shorter slab (Fig. 1(c)) can be written

$$M_{21} = T_X T_1 T_{L1} T_2 T_Y, \tag{11}$$

24 December 2023 12:54:29

where

$$T_u = \begin{bmatrix} \alpha_u & 0 \\ 0 & 1/\alpha_u \end{bmatrix}, \quad \alpha_u = e^{-\gamma_0 L_{0u}}, \tag{12}$$

and L_{01} and L_{02} are arbitrary lengths of air-filled sections inside the measurement cell in Fig. 1(c). Then, using Eqs. (1) and (11), we obtain

$$M_{21}M_2^{-1} = T_X T_1 T_{L1} T_2 T_{L2}^{-1} T_X^{-1}. \tag{13}$$

It is clear from Eq. (13) that $Tr(M_{21}M_2^{-1}) = Tr(T_1 T_{L1} T_2 T_{L2}^{-1})$.[18–20,29] Next, using Eqs. (3), (11), and (12), we find an objective function

$$F_{obj}(\Gamma) = \Lambda_1 \Gamma^4 + \Lambda_2 \Gamma^2 + \Lambda_3 = 0, \tag{14}$$

where

$$\Lambda_1 = \frac{T_{s1}^2}{\alpha_1 \alpha_2} + \alpha_1 \alpha_2 T_{s2}^2 - \Lambda_0, \quad \Lambda_0 = Tr\left(M_{21}M_2^{-1}\right) T_{s1} T_{s2}, \tag{15a}$$

$$\Lambda_2 = (1 + T_{s1}^2 T_{s2}^2)\left(\frac{\alpha_1^2 + \alpha_2^2 - \alpha_1^2 \alpha_2^2 - 1}{\alpha_1 \alpha_2}\right) - (T_{s1}^2 + T_{s2}^2)\left(\frac{\alpha_1^2 + \alpha_2^2}{\alpha_1 \alpha_2}\right) + 2\Lambda_0, \tag{15b}$$

$$\Lambda_3 = \frac{T_{s2}^2}{\alpha_1 \alpha_2} + \alpha_1 \alpha_2 T_{s1}^2 - \Lambda_0. \tag{15c}$$

It is obvious from Eq. (14) and (15) that F_{obj} is a function of only Γ since using Eqs. (9) and (4), T_{s1} and T_{s2} can readily be expressed as

$$T_{s1} = \left(\lambda_{(1,2)}\right)^{L_1/\Delta L}, \quad T_{s2} = \left(\lambda_{(1,2)}\right)^{L_2/\Delta L}. \tag{16}$$

As a result, using $Tr(M_1 M_2^{-1})$ and $Tr(M_{21}M_2^{-1})$ we can determine Γ from Eq. (14). Because there are two roots for Γ in Eq. (14), the correct root can be chosen by imposing the constraint $|\Gamma| \leq 1$ (or $\Re e\{Z_s\} \geq 0$) for passive samples and continuity of Γ over frequency. Finally, the ε_r and μ_r can analytically be determined by using Eqs. (4), (5), (9), and (14) as

$$\mu_r = \frac{\gamma}{\gamma_0}\left(\frac{1+\Gamma}{1-\Gamma}\right), \quad \varepsilon_r = \frac{1}{\mu_r}\left(\frac{\gamma}{\gamma_0}\right)^2. \tag{17}$$

III. ON ACCURACY AND STABILITY OF THE PROPOSED METHOD

In the derivation of the objective function in Eq. (14) it is tacitly assumed that $\alpha_1 \neq 1$ and $\alpha_2 \neq 1$. It is instructive then to evaluate what happens when a) $\alpha_1 = \alpha_2 = 1$ and b) $\alpha_1 = \alpha_2 = \alpha_0$ where $\alpha_0 \neq 1$. We will also demonstrate how the correct root for $\lambda_{(1,2)}$ and $\gamma_{(1,2)}$ from Eqs. (9) and (10) can be selected. Finally, we will investigate the stability of the derivations for $\gamma_{(1,2)}$ in Eq. (10) and Γ in Eq. (14) for different values of S-parameters.

A. Analysis of special cases for α_1 and α_2

We first consider the case when $\alpha_1 = \alpha_2 = 1$, corresponding to the case in which the shorter slab with length L_1 fills completely the measurement cell in Fig. 1(c). Although this case is already taken into consideration in the determination of γ in Subsection II B, it is important for two reasons: 1) it verifies the derivation of the objective function in Eq. (14), and 2) it underlines the basic idea behind the constitutive parameters (ε_r and μ_r simultaneously) determination.

Substituting $\alpha_1 = \alpha_2 = 1$ into Eqs. (14) and (15), we obtain with the assumption of $\Gamma \neq \mp 1$

$$\Lambda_1^{(1)} = T_{s1}^2 + T_{s2}^2 - \Lambda_0, \quad \Lambda_2^{(1)} = -2\Lambda_1^{(1)}, \quad \Lambda_3^{(1)} = \Lambda_1^{(1)}, \tag{18a}$$

$$Tr(T_{L1}T_{L2}^{-1}) = \left(\frac{T_{s1}}{T_{s2}} + \frac{T_{s2}}{T_{s1}}\right), \tag{18b}$$

24 December 2023 12:54:29

where $\Lambda_1^{(1)}$, $\Lambda_2^{(1)}$, and $\Lambda_3^{(1)}$, respectively, correspond to the Λ_1, Λ_2, and Λ_3 values when $\alpha_1 = \alpha_2 = 1$. Here, it is clear that Eq. (18b) will reduce to Eq. (9), which accordingly verifies the derivation of $F_{obj}(\Gamma)$, and that this case does not give any information about the value of a physical Γ ($|\Gamma| \leq 1$).

We next consider the case when $\alpha_1 = \alpha_2 = \alpha_0$ where $\alpha_0 \neq 1$, corresponding to the case of the shorter slab symmetrically positioned into the measurement cell (the same air regions between the end surfaces of the shorter slab and the terminals of the cell) in Fig. 1(c). Reflecting the condition $\alpha_1 = \alpha_2 = \alpha_0$ where $\alpha_0 \neq 1$ into Eqs. (15a)-(15c) we determine

$$\Lambda_1^{(2)} = \frac{T_{s1}^2}{\alpha_0^2} + \alpha_0^2 T_{s2}^2 - \Lambda_0, \tag{19a}$$

$$\Lambda_2^{(2)} = -\frac{1}{\alpha_0^2}\left[\left(1-\alpha_0^2\right)^2 + T_{s1}^2 T_{s2}^2\left(1+\alpha_0^4\right)\right] + 2\Lambda_0, \tag{19b}$$

$$\Lambda_3^{(2)} = \frac{T_{s2}^2}{\alpha_0^2} + \alpha_0^2 T_{s1}^2 - \Lambda_0. \tag{19c}$$

where $\Lambda_1^{(2)}$, $\Lambda_2^{(2)}$, and $\Lambda_3^{(2)}$, respectively, correspond to the Λ_1, Λ_2, and Λ_3 values when $\alpha_1 = \alpha_2 = \alpha_0$ where $\alpha_0 \neq 1$.

Because using Eqs. (10) or (18b) we can determine at most either ε_r or μ_r via the complex propagation constant γ, we also need to measure Γ to extract ε_r and μ_r simultaneously. It is apparent from Eqs. (19a)-(19c) that $\Lambda_1^{(2)}$, $\Lambda_2^{(2)}$, and $\Lambda_3^{(2)}$ are all linearly independent from one another so that their substitution into Eq. (14) will not allow the factoring out of the Γ term. Therefore, this case gives some information about Γ. As a result, considering these two special cases, we conclude that the sufficient condition for simultaneous ε_r and μ_r determination in LL methods is to measure raw S-parameters of two measurement cells which are completely and partially (symmetrically or asymmetrically) loaded by the two identical unknown slabs with different lengths ($L_1 \neq L_2$).

B. Solving the ambiguity in the selection of the correct propagation constant

It is obvious from Eq. (9) that $\lambda_{(1,2)}$ represents both forward and backward traveling waves inside the MM slab. In this circumstance, it is difficult to discern which eigenvalue, λ_1 or λ_2 (in Green's function terminology), corresponds to forward or backward traveling waves at a given frequency. To resolve this problem, a simple technique using the comparison of $\lambda_{(1,2)}$ at different frequencies was introduced.[23] In applying this technique, for the first two lowest frequencies in the band, the positive solution of Eq. (9) is arbitrarily retained and plotted in the complex plane. For each of next frequencies, the two possible solutions in Eq. (9) are tested and only the one which ensures a monotonic variation of $\lambda_{(1,2)}$ in the complex plane is taken as the correct solution. This technique resembles to similar ones in the literature[3,8,31–34] and is based on the principle of causality of physical (non-anticipative) systems in which the system response is directly dependent upon past and present values of the input.

C. Stability analysis for the complex permittivity and permeability determination

Because the derivations for ε_r and μ_r depend on $M_1 M_2^{-1}$ and $M_{21} M_2^{-1}$, we have to monitor the effects of measurement uncertainties on ε_r and μ_r determination. Using Eq. (2), we can express $Tr(M_1 M_2^{-1})$ as

$$Tr(M_1 M_2^{-1}) = \frac{S_{12}^{(1)} S_{21}^{(1)} + S_{12}^{(2)} S_{21}^{(2)} - S_{11}^{(1)}\left(S_{22}^{(1)} + S_{11}^{(2)}\right) - S_{22}^{(2)}\left(S_{11}^{(2)} + S_{22}^{(1)}\right)}{S_{21}^{(1)} S_{12}^{(2)}}. \tag{20}$$

When both $S_{11}^{(u)}$ and $S_{22}^{(u)}$ approach zero in Eq. (20), the value of $Tr(M_1 M_2^{-1})$ will not go to zero or infinity as in the case of broadband constitutive parameters determination by the methods[3,8,10] (i.e., inadequacy of retrieval procedures[35,36]), and thus will be stable. In addition, it is well-known that the phase uncertainty of measured reflection S-parameters ($S_{11}^{(u)}$ and $S_{22}^{(u)}$) increases significantly

24 December 2023 12:54:29

when $S_{11}^{(u)}$ and $S_{22}^{(u)}$ simultaneously or separately approach zero. This situation results in a large ripple in the extracted ε_r and μ_r[36] (or anti-resonant behavior[35]) by most S-parameter techniques in the literature since the phase uncertainty in $S_{11}^{(u)}$ and/or $S_{22}^{(u)}$ is multiplied by $1/|S_{11}^{(u)}|$ and/or $1/|S_{22}^{(u)}|$ in the process of extracting ε_r and μ_r.[3,8,10] Here, the vertical bars on each side of a quantity denote its magnitude. On the other hand, it is expected that the proposed method will extract more smoother ε_r and μ_r over a broad band since the effect of phase uncertainty is already mitigated by the amplitudes of reflection S-parameters in Eq. (20). Because the WCM and ABCD matrix representations preclude both $S_{21}^{(u)}$ and $S_{12}^{(u)}$ from approaching zero, the derivations of ε_r and μ_r will be stable by the proposed method. However, when the amplitudes of $S_{21}^{(u)}$ and/or $S_{12}^{(u)}$ become less than approximately -30 dB (depending on the accuracy of measuring instrument), the uncertainties in amplitudes and phases of $S_{21}^{(u)}$ and $S_{12}^{(u)}$ will greatly increase, and this circumstance may adversely affect ε_r and μ_r extraction. As a result, the derivations for ε_r and μ_r from Eqs. (10) and (14) are generally effective and suitable for high-to-low-loss (but not very high-loss) MM slabs.

IV. RESULTS

For validation of the proposed method, in this section we consider a MM slab with SRRs in rectangular or circular form. This MM slab structure is one of the mostly studied MM slabs in the literature.[3,4,8–10,17–20] The cell of the analyzed slab, as shown in Fig. 2(a) – slightly differing from that in,[3,4] is assumed to be in cubical form ($a_y = a_z = L = 4$ mm) and has the following features. The substrate onto which the metal strips of SRRs are placed has a complex permittivity of $\varepsilon_s = 4.4 - i0.15$, a thickness of $t = 0.25$ mm, and an area of 4×4 mm^2. Strips are assumed to be copper [5.8×10^7 (S/m)] with a thickness of 17 μm. The outer ring length is $l = 2.2$ mm and both rings have a linewidth of $w = 0.2$ mm. While the slit gap is $g = 0.22$ mm for both rings, the separation distance between inner and outer rings is $s = 0.15$ mm. While the MM slab with length $L_1 = 4.0$ mm is obtained by periodic arrangement of the cell in Fig. 2(a) in the y and z directions with periods $a_y = 4.0$ mm and $a_z = 4.0$ mm, the MM slab with length $L_2 = 8.0$ mm is obtained by the cascaded connection of two identical MM slabs with lengths $L_1 = 4.0$ mm in the x direction (wave propagation direction).

S-parameters simulations are performed by a commercial 3-D full electromagnetic simulation software (CST Microwave Studio©[37]). In the simulations, electric (magnetic) boundary conditions for which tangential components of electric (magnetic) fields are zero are applied at xy (xz) planes. To ensure periodicity of the unit cell (Fig. 2(a)) in the yz plane as well as a wave propagating in the x direction, waveguide ports are positioned over yz planes. Fig. 2(b) demonstrates magnitudes of the simulated S-parameters of the investigated SRR MM slabs with $L_1 = 4.0$ mm and $L_2 = 8.0$ mm (simulated S-parameters for the configurations in Fig. 1(a) and 1(b), respectively). For simplicity, phases of the these simulated S-parameters as well as S-parameters of the configuration in Fig. 1(c) are not shown. It is seen from Fig. 2(b) that both of the investigated SRR MM slabs with lengths L_1 and L_2 resonate around 11.0 GHz, at which fast variation of S-parameters is notable.

It is a well-known fact that for the analyzed wave incidence (wave propagation in x direction and electric field in z direction), the cell in Fig. 2(b) behaves as an isotropic MM slab (no coupling between electric and magnetic fields[4,10]), characterized by both ε_r and μ_r or both z and n [Eqs. (4) and (5)]. For validation of our method, we first substitute the simulated S-parameters, corresponding to the configurations in Fig. 1(a)-1(c), into Eq. (2). Then, we calculate the matrix multiplications $M_{21}M_2^{-1}$ and $M_1M_2^{-1}$. Next, we find γ from Eq. (10) and Γ from Eq. (14). Using Eqs. (17) and (4), we finally extract n, z, ε_r, and μ_r values, as shown in Figs. 3 and 4, of the analyzed MM slab by applying the proposed method (PM). The same figures also illustrate the extracted n, z, ε_r, and μ_r parameters of the MM slab with length $L_1 = 4.0$ mm by the general method (GM) in.[3,10,17] We have the following two important points drawn from the dependencies in Figs. 3 and 4. First, each extracted electromagnetic parameter by the proposed method is in good harmony with that by the general method. Second, while extracted ε_r'' by the general method is less than zero over approximately 10.3-11.0 GHz (as seen from the inset in Fig. 4(a)), that by the proposed method is greater than zero over the whole analyzed frequency band (5.0-15.0 GHz). It is a well-established

24 December 2023 12:54:29

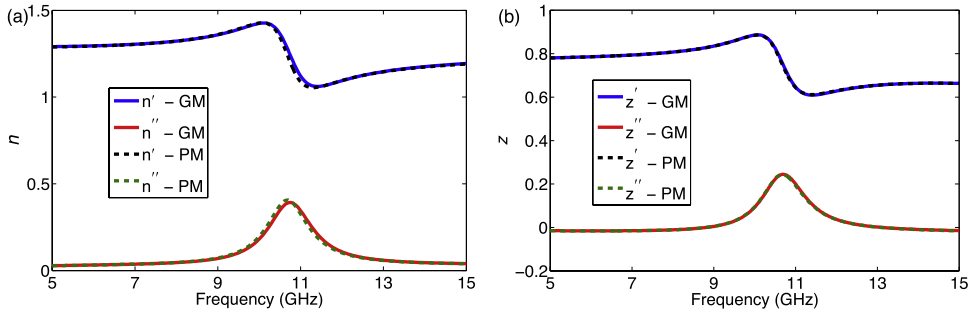


FIG. 3. Real and imaginary parts of the retrieved (a) refractive index (n) and (b) the normalized wave impedance (z) by the general method (GM) in Refs. 3, 10, and 17 and the proposed method (PM).

fact that for a passive medium such as that we consider in our paper in Fig. 2(a), ε_r'' (and μ_r'') must all be positive in the whole frequency range.[3,8,10,16,17,35,38] In a recent study,[35] it has also been shown that non-physical anti-resonant behavior [a decay in the electromagnetic property with increasing frequency (e.g., a negative slope of ε_r' between 10.3-11.0 GHz in Fig. 4(a)) and an increase in power gain around the resonance band (e.g., $\varepsilon_r'' < 0$ between 10.3-11.0 GHz in Fig. 4(a))] of extracted electromagnetic properties comes from not periodicity of MM slabs but from in-complete adequacy of retrieval procedures. In addition, in another study[38] it has also been demonstrated that this non-physical behavior of electromagnetic properties of MM slabs can be remedied by fitting the simulated S-parameters to those obtained from the Lorentz/Drude effective medium models. As a result, for the tested MM slab in Fig. 2(a) we note that our proposed method not only extracts physically acceptable electromagnetic properties but also eliminates the need for the fitting process for accurate electromagnetic properties.

In the calculation of the frequency-dependent parameters in Figs. 3 and 4 we assumed that measurement error sources (incorrect reference-planes, source and load match errors, errors due to mismatched connections, transitions between connecting cables and horn antennas, contact structures, embedded devices) have no effect on electromagnetic properties extracted by both methods. Now, we consider the effect of a shift in positions of reference planes [planes or surfaces to which the setup is assumed to be calibrated; e.g., to the left and right terminals of S_1 in Fig. 1(a)] on n, z, ε_r, and μ_r parameters. For simplicity, it is assumed in this analysis that while there is no shift in the reference-plane on the right surface of the MM slab, there is a -1 mm shift in the reference-plane on the left surface of the MM slab. In the extraction of electromagnetic properties by the GM method, the effect of a shift in the left reference-plane is reflected into the analysis by multiplying the reflection and transmission S-parameters for the configuration in Fig. 1(a) with $\exp(+2\gamma_0)$ and $\exp(+\gamma_0)$, respectively (please refer to Eqs. (11) and (12) for more details). Figs. 5 and 6 illustrate the retrieved electromagnetic parameters of the analyzed SRR MM slab using the GM method (from S-parameters of only the MM slab with length $L_1 = 4.0$ mm) and the PM method.

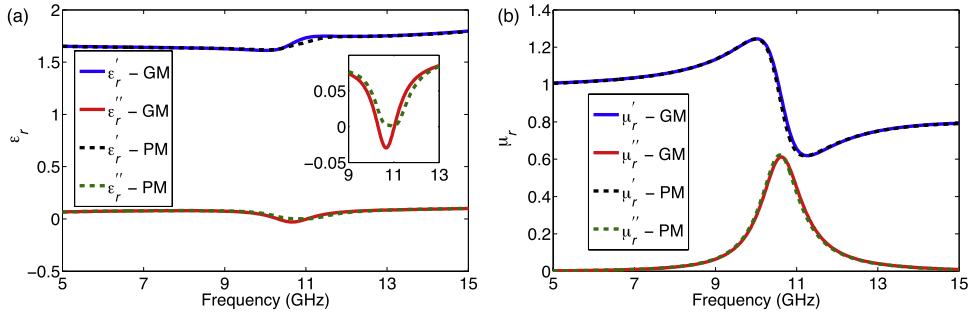


FIG. 4. Real and imaginary parts of the retrieved (a) relative complex permittivity (ε_r) and (b) relative complex permeability (μ_r) by the general method (GM) in Refs. 3, 10, and 17 and the proposed method (PM).

24 December 2023 12:54:29

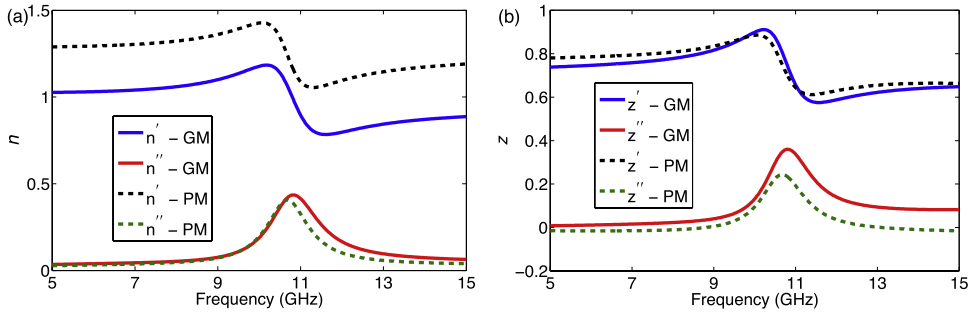


FIG. 5. Real and imaginary parts of the retrieved (a) refractive index (n) and (b) the normalized wave impedance (z) by the general method (GM) in Refs. 3, 10, and 17 and the proposed method (PM) when there is an offset (-1 mm) in the reference-plane position on left side of the MM slab.

By comparison with the dependencies in Figs. 3 and 4, it seen from the dependencies in Figs. 5 and 6 that an absolute shift of 1 mm (a generally acceptable level of measurement error at microwave frequencies) drastically alters actual dependencies of electromagnetic parameters retrieved by the general method.[3,10,17] This is because MM structures are resonating structures whose response sharply changes around resonance frequency. The same amount of shift, nonetheless, does not affect the same frequency-dependent parameters extracted by the proposed method. Furthermore, we note that the offset in the left reference-plane position results in a non-physical ε_r'' extracted by the GM method over a broader band (10.3-15.0 GHz) than that (10.3-11.0 GHz) when there is no offset. As a result, the dependencies in Figs. 5 and 6 clearly indicate the importance of a retrieval method resistant to undesired measurement errors arising from a shift in reference-plane positions.

To test the proposed method for other systematic measurement errors such as source and load match errors, errors due to mismatched connections, and imperfection of the used calibration kit, we have considered various T_X and T_Y square matrices in Eqs. (1) and (11). We note from this analysis that our proposed method is resistant and immune to those errors and retrieves accurate constitutive parameters of the test MM slab because our proposed method eliminates the effect of unknown error matrices T_X and T_Y in Eqs. (11) and (13) from determination of electromagnetic parameters,[25,28,29] as discussed in Subsection II C.

V. CONCLUSIONS

We have proposed a calibration-independent method for determination of complex permittivity and complex permeability of isotropic homogeneous MM slabs. We think that such a method, capable of extracting the constitutive parameters, has been proposed for the first time in the literature. Its advantage is that it removes or eliminates measurement errors of various origins arising

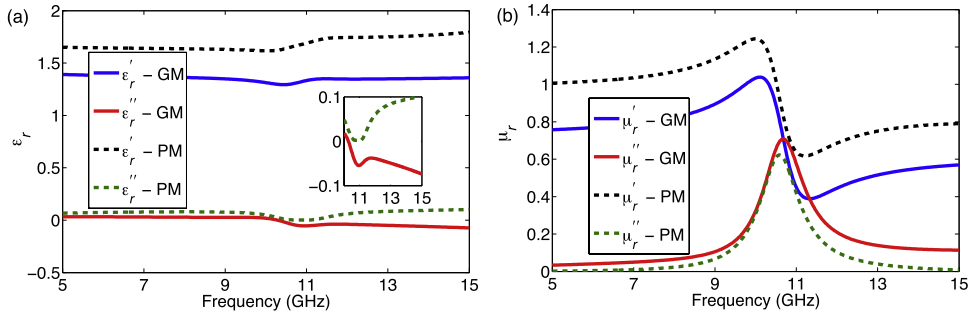


FIG. 6. Real and imaginary parts of the retrieved (a) relative complex permittivity (ε_r) and (b) relative complex permeability (μ_r) by the general method (GM) in Refs. 3, 10, and 17 and the proposed method (PM) when there is an offset (-1 mm) in the reference-plane position on left side of the MM slab.

24 December 2023 12:54:29

from incorrect reference-planes, source and load match errors, errors due to mismatched connections, transitions between connecting cables and horn antennas, contact structures, embedded devices. The idea behind how the constitutive parameters are retrieved is through some illustrative cases. In addition, the accuracy of the proposed method is analyzed by letting the reflection S-parameters approach zero. We have tested the proposed method by using simulated S-parameters of a MM slab with SRRs and noted for the tested slab that while our proposed method removes the so-called antiresonance problem as well as the problem of measurement errors, the method widespreadly used in the literature has both of these problems in different levels.

ACKNOWLEDGMENTS

Authors, U. C. Hasar, G. Buldu, M. Bute, T. Karacali, and M. Ertugrul, would like to express their thanks to the Scientific and Technological Research Council of Turkey (TUBITAK) under the project Grant Number 112R032 for supporting this study. U. C. Hasar also sends special thanks to the Science Academy of Turkey (the Young Scientists Award in 2014) for supporting his studies.

[1] J. B. Pendry, Phys. Rev. Lett. **85**, 3966 (2000).
[2] J. B. Pendry, D. Schuring, and D. R. Smith, Science **312**, 1780 (2006).
[3] D. R. Smith, S. Schultz, P. Markos, and C. M. Soukoulis, Phys. Rev. B **65**, 195104 (2002).
[4] R. Marqués, F. Medina, and R. Rafii-El-Idrissi, Phys. Rev. B **65**, 144440 (2002).
[5] C. R. Simovski and S. He, Appl. Phys. Lett. **311**, 254 (2003).
[6] M. Choi, S. H. Lee, Y. Kim, S. B. Kang, J. Shin, M. H. Kwak, K.-Y. Kang, Y.-H. Lee, N. Park, and B. Min, Nature **470**, 369 (2011).
[7] Z. Li, M. Mutlu, and E. Ozbay, J. Opt. **15**, 023001 (2013).
[8] X. Chen, T. M. Grzegorczyk, B.-I. Wu, J. Pacheco, Jr., and J. A. Kong, Phys. Rev. E **70**, 016608 (2004).
[9] X. Chen, B.-I. Wu, J. A. Kong, and T. Grzegorczyk, Phys. Rev. E. **71**, 046610 (2005).
[10] Z. Li, K. Aydin, and E. Ozbay, Phys. Rev. E **79**, 026610 (2009).
[11] R. Zhao, T. Koschny, and C. M. Soukoulis, Opt. Express **18**, 14553 (2010).
[12] D. R. Smith, D. C. Vier, T. Koschny, and C. M. Soukoulis, Phys. Rev. E **71**, 036617 (2005).
[13] T. Driscoll, D. N. Basov, W. J. Padilla, J. J. Mock, and D. R. Smith, Phys. Pev. B **75**, 115114 (2007).
[14] C. Menzel, C. Rocksthul, T. Paul, and F. Lederer, Phys. Pev. B **77**, 195328 (2008).
[15] A. Andryieuski, R. Malureanu, and A. V. Lavrinenko, Phys. Rev. B **80**, 193101 (2009).
[16] S. Kim, E. F. Kuester, C. L. Holloway, A. D. Scher, and J. Baker-Jarvis, IEEE Trans. Antennas Propag. **59**, 2226 (2011).
[17] U. C. Hasar, J. J. Barroso, C. Sabah, Y. Kaya, and M. Ertugrul, J. Opt. Soc. Am. B **30**, 1058 (2013).
[18] U. C. Hasar and J. J. Barroso, J. Electromagn. Waves Appl. **25**, 2110 (2011).
[19] U. C. Hasar, J. J. Barroso, and M. Ertugrul, J. Electromagn. Waves Appl. **26**, 54 (2012).
[20] U. C. Hasar and J. J. Barroso, J. Infrared Milli. Terahertz Waves **33**, 218 (2012).
[21] A. Enders, IEEE Trans. Microw. Theory Tech. **MTT-37**, 598 (1989).
[22] M. D. Janezic and J. A. Jargon, IEEE Microwave Guided Wave Lett. **9**, 76 (1999).
[23] J. A. Reynoso-Hernandez, IEEE Microw. Wireless Compon. Lett. **13**, 351 (2003).
[24] N. J. Farcich, J. Salonen, and P. M. Asbeck, IEEE Trans. Microw. Theory Tech. **56**, 2963 (2008).
[25] K.-H. Baek, H.-Y. Sung, and W. S. Park, IEEE Microwave Guided Wave Lett. **5**, 3 (1995).
[26] U. C. Hasar, I. Y. Ozbek, E. A. Oral, T. Karacali, and H. Efeoglu, Opt. Express **20**, 22208 (2012).
[27] T. Karacali, U. C. Hasar, I. Y. Ozbek, E. A. Oral, and H. Efeoglu, J. Lightwave Technol. **31**, 295 (2013).
[28] C. Wan, B. Nauwelaers, and W. De Raedt, IEEE Microwave Guided Wave Lett. **8**, 58 (1998).
[29] U. C. Hasar and O. Simsek, J. Phys. D: Appl. Phys. **42**, 075403 (2009).
[30] M. J. Akhtar, L. E. Feher, and M. Thumm, IEEE Trans. Microw. Theory Tech. **57**, 458 (2009).
[31] J. J. Barroso and U. C. Hasar, J. Infrared Milli. Terahz Waves **32**, 857 (2011).
[32] J. J. Barroso and U. C. Hasar, J. Infrared Milli. Terahertz Waves **33**, 237 (2012).
[33] U. C. Hasar, J. J. Barroso, C. Sabah, and Y. Kaya, Prog. Electromagn. Res. **129**, 405 (2012).
[34] Z. X. Cao, F. G. Yuan, and L. H. Li, AIP Advances **4**, 067115 (2014).
[35] P. Alitalo, A. C. Culhaoglu, C. R. Simovski, and S. A. Tretyakov, J. Appl. Phys. **113**, 224903 (2013).
[36] U. C. Hasar, J. J. Barroso, Y. Kaya, M. Bute, and M. Ertugrul, J. Electromagnetic Waves Appl. **28**, 903 (2014).
[37] CST Microwave Studio. Version 2014. Darmstadt (Germany): CST GmbH.
[38] G. Lubkowski, R. Schuhmann, and T. Weiland, Microw. Opt. Technol. Lett. **49**, 285 (2007).

24 December 2023 12:54:29